Supporting information for

In vivo real-time simultaneous examination of drug kinetics at two separate locations using boron doped diamond microelectrodes

Ai Hanawa,[1#] Genki Ogata,[2#] Seishiro Sawamura,[2] Kai Asai,[1] Sho Kanzaki,[3] Hiroshi Hibino,[2*] Yasuaki Eianga[1*]

[1]Department of Chemistry, Keio University, 3-14-1 Hiyoshi, Yokohama 223-8522, Japan

[2]Department of Molecular Physiology, School of Medicine, Niigata University, Niigata 951-8510, Japan

[3]Department of Otolaryngology, School of Medicine, Keio University, 35 Shinanomachi, Shinjuku-ku, Tokyo 160-8582, Japan

[#]Contributed equally

*Corresponding authors

Contents:

1. Experimental Methods

Preparation of boron-doped diamond (BDD) electrodes

The method used to prepare the BDD electrodes was similar to that given in our previous reports.[22, 23, 30] Briefly, polycrystalline BDD films were deposited on silicon wafers and on tungsten wires to fabricate plate electrodes and microelectrodes, respectively. For microelectrodes, initially, the 50 or 100 μm diameter tungsten wires were electropolished in a solution of 2 M KOH to achieve a conical shape. The deposition was done in a microwave plasma-assisted chemical vapor deposition (MPCVD) system (AX5250M, Cornes Technologies, Ltd.), with plasma powers of 5.0 kW and 3.0 kW applied for 6 h and 2h with deposition pressures of 100 Torr and 60 Torr, respectively. A mixture of acetone and trimethoxyborane was used for the carbon and boron sources with a boron/carbon ratio of 1%. The surface morphology and crystalline structure was characterized using scanning electron microscopy (SEM) (JCM-6000 plus, JEOL, Ltd.) (Figure S11(a)(b)). The film quality was confirmed by Raman spectroscopy (Acton SP2500, Princeton Instruments, Inc.) (Figure S11(c)(d)). Both of the Raman spectra (of the plate and the microelectrode) showed peaks of the center zone optical phonon of diamond (sp^3) at 1332 cm^{-1} on the shoulder of a band at around 1220 cm^{-1}, which can be observed in metallic, heavily-doped BDD.[45] The BDD microelectrodes were insulated with glass capillaries to define the electrode surface area. A capillary (G-100, Narishige) was pulled by capillary puller (PC-10, Narishige). The tip of the capillary was then cut by microforge (MF-900, Narishige) to cover the BDD needle with the tip extruding by ca. 100–200 μm. The capillary-covered BDD needle was heated at ca. 700 ºC for 30 s in argon atmosphere. The capillary was evacuated by a diaphragm pump (DIVAC 0.6L, Lenbold) during the heating. This procedure was necessary for a tight seal between the BDD and the glass capillary (Figure SX: below). Then, copper wires were connected to the microelectrodes with silver paste. The details of the preparation have been described previously.[46] The sizes of the conducting tips of the electrodes were < 30 μm in diameter and 50-300 μm in length.

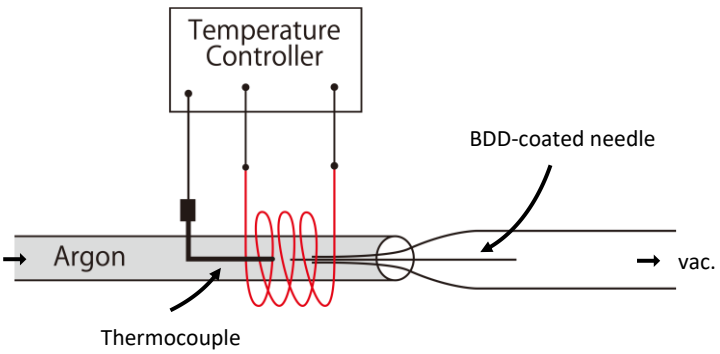

Figure SX. Insulation of BDD microelectrode in glass capillary.

Chemicals

Methylcobalamin and potassium hexacyanoferrate(II) trihydrate ($K_4[Fe(CN)_6]$) were purchased from FUJIFILM Wako Pure Chemical Corporation and used without any purification. A 0.1 M phosphate buffer (PB) solution with pH 7.4 was used as the electrolyte. This solution contained 19 mM sodium dihydrogen phosphate (NaH_2PO_4) and 81 mM sodium hydrogen phosphate (Na_2HPO_4). A 1 M aqueous solution of sulfuric acid (H_2SO_4) was used to clean the BDD electrode by cathodic reduction. All the solutions were prepared with pure water supplied from DIRECT-Q 3 UV (Merck Millipore Corp.) with a specific resistivity of 18.2 MΩ·cm.

Preparation of reference and counter electrodes

The reference and counter electrodes used *in vitro* with the plate BDD electrodes were prepared as follows. The reference electrode was an Ag/AgCl (HS-205C, DKK-TOA Corp.) electrode connected to a salt bridge filled with a saturated solution of potassium chloride (KCl). A coiled Pt wire (0.5 mm in diameter) was used as the counter electrode. A BDD plate electrode was also selected as the counter electrode to conduct cathodic reduction in 1 M H_2SO_4.

The fabrication processes for the reference and counter electrodes used for the *in vivo* measurements are described elsewhere.[30] Briefly, a double-barreled glass capillary (World Precision Instruments Inc., Sarasota, FL, USA) was pulled by means of a micropipette puller (P-97; Sutter Instrument, Novato, CA, USA). The inside of the tip (~200-μm diameter for each) of each barrel was packed with 1.5% w/v agar dissolved in phosphate-buffered saline (PBS). This solution contained 137 mM sodium chloride (NaCl), 8.1 mM sodium hydrogen phosphate (Na_2HPO_4), 2.68 mM potassium chloride (KCl), and 1.47 mM potassium dihydrogen phosphate (KH_2PO_4) at pH 7.4. To prepare the counter electrode, a platinum wire (500-μm diameter) was placed into one of the barrels containing the PBS. For the reference electrode, an Ag/AgCl wire (500-μm diameter) was inserted into the other barrel, which was backfilled with a 3 M KCl solution.

***In vitro* electrochemical measurements**

Electrochemical measurements were carried out using a potentiostat (ALS 852cs, BAS Inc.) controlled by a laptop computer. Initially, cyclic voltammetry (CV) was conducted with the potentiostat using a single-compartment three-electrode polytetrafluoroethylene (PTFE) cell with an Ag/AgCl (saturated KCl) reference electrode and a coiled Pt wire counter electrode. The electrical contacts for the electrochemical measurements were made by connecting copper wires to the BDD surface with silver paste. The BDD (Pt and GC) electrode was fixed with an O-ring (electrode area: 0.36 cm^2) and connected to the potentiostat through a copper plate placed under the working electrode.

For continuous measurements, a BDD microelectrode was used as the working electrode. The

3 electrodes (working electrode, counter electrode and reference electrode) were immersed in a beaker containing 5 ml of phosphate buffer solution (Figure S4). Three different measurement protocols were examined. For each protocol, stock solutions of methylcobalamin were added to the PB solution in the beaker, which was then stirred with a magnetic bar for 3 seconds.

Protocol A is a single step process. The potential was fixed at −0.7 V (vs. Ag/AgCl), and the current monitored every 4 seconds. The background current increased gradually even without injection of methylcobalamin (Figure 2a2), and the current after administration of the methylcobalamin was unstable, not reflecting the methylcobalamin concentration (Figure 2(a3)). Protocol B is a two-step process. In order to stabilize the background current, a positive potential (+ 1.4 V (vs. Ag/AgCl)) was applied for 2 seconds before the measurements at −0.7 V (vs. Ag/AgCl). Protocol C is a three-step process. After the measurements at −0.7 V (vs. Ag/AgCl), −2.0 V (vs. Ag/AgCl) was applied for 1 second.

Then, each of the potentials applied in Protocol C, i.e. the positive potential (+1.4 V), measurement potential (−0.7 V), and the negative potential (−2.0 V) were optimized. First, the applied positive potential was optimized by making measurements with the positive potential being varied from 0.0 V to +1.5 V (Figure S6). Next, the measurement potential for the data collection, i.e., the reduction potential of methylcobalamin, was optimized from −0.6 V (vs. Ag/AgCl) to −1.0 V (vs. Ag/AgCl) (Fig. S7). Then, the applied negative potential was optimized from −1.0 V (vs. Ag/AgCl) to −2.0 V (vs. Ag/AgCl) (Figure S8). All the measurements were conducted at room temperature (~25℃).

Ethical statement for animal experiments

The protocol for animal experiments was approved by the Animal Care and Use Committee and President of Niigata University (Permission Number: SA00118). *In vivo* measurements were performed in accordance with the Japanese Animal Protection and Management Law and under the supervision of the committee. The guinea pigs were housed in the animal facility at the Niigata University School of Medicine. The guinea pigs were kept on a 12-h light / 12-h dark cycle and all experiments were carried out during the light cycle. Food and water were provided *ad libitum*. All animal handling and reporting comply with the ARRIVE guidelines.[47]

***In vivo* measurements of methylcobalamin**

Each BDD microelectrode was used for only one series of *in vivo* measurements in a guinea pig and was not used in other animals. Before being used in an *in vivo* experiment, the microelectrode was immersed in a 1 M H_2SO_4 solution and 3.0 V (vs. Ag/AgCl) was applied for 30 s and subsequently −4.0 V (vs. Ag/AgCl) for 1200 s. With these anodic and cathodic pretreatments, the BDD surface was rid of any impurities and dominated by hydrogen termination.[48,49] The electrode was then

subjected to a cyclic voltammetry protocol (sweep rate, 0.1 V/s; potential window, −1.0 V to 1.5 V (vs. Ag/AgCl); and initial potential, 0.0 V (vs. Ag/AgCl)) in PB solution until the background signal became stable. Thereafter, a calibration curve for the microelectrode was determined *in vitro*. Any electrode which failed to have a slope ≥ 1.0 was discarded.

Healthy male Hartley guinea pigs (350–700 g, 2–12 weeks old; SLC Inc., Hamamatsu, Japan), the hearing levels of which were evaluated in advance by Preyer's reflex test and confirmed to be normal, were used for the *in vivo* experiments. Urethane (1.5 g kg^{-1}, Sigma-Aldrich Japan, Tokyo, Japan) was intraperitoneally injected into the animals for deep anesthesia. The depth of the anesthesia was continuously monitored with a toe pinch, the corneal reflex, and the respiratory rate. During the recording, the body temperature was maintained at 37 °C on a heating blanket (BWT-100A, BioResearch Center, Nagoya, Japan). To inject methylcobalamin, an ethylene tetrafluoroethylene tube was inserted into the right external jugular vein of each guinea pig. 5 mg of methylcobalamin was dissolved in 1 ml of PB solution immediately before being injected into each guinea pig for the *in vivo* measurements; the dosage was 10 mg kg^{-1} for each guinea pig.

The guinea pigs were prepared as follows. These preparations are based on those used in our earlier studies.[30,50] The cochlea on the left side was exposed by means of a ventrolateral approach and a hole (~800-μm diameter) was made in the bony wall of the basal turn. In addition, the skin of the right hind leg was cut by surgical scissors and a small area of the gracilis muscle (~1 cm^2) was exposed. For the cochlea, the BDD microelectrode was inserted through the hole into the scala tympani filled with the perilymph (Figure 4c). The tip of the double-barreled microcapillary containing the reference and counter electrodes was placed in the vicinity of the BDD microelectrode in the same cochlear compartment. Then, the other BDD microelectrode was inserted into the muscle. The manipulators and electrode holders (MN-153, Narishige, Japan) were used to fix the electrodes in place for the cochlea and muscle. The protocol and procedures for cyclic voltammetry assays under controlled conditions and those for chronoamperometry monitoring of the methylcobalamin concentration in the cochlear perilymph and the leg muscle are described in the 'Results and Discussion' section of the *main text*, and the results are shown in Figure 4, and Figure S10. The solution containing methylcobalamin was injected for a period of 60 s into the tube attached to the vein 30 min after starting the electrochemical recording. The average current at –0.7 V (vs. Ag/AgCl) was measured for 10 min prior to injecting the solution. This average is defined as the baseline current. Then, the difference between this and the current recorded during the remainder of the experiment was converted to the methylcobalamin concentration using the *in vitro* calibration curve unique to each BDD microelectrode. After the measurements, the animals were euthanized by means of an overdose of pentobarbital sodium (400 mg kg^{-1}).

Six guinea pigs in total were used in the *in vivo* experiments. However, the BDD microelectrode in the leg muscle of one guinea pig broke during recording. Furthermore, it is likely

that in 2 of the experiments the surface of the surgically exposed leg muscle lost moisture, so that, in one case, the background noise level increased significantly, and, in the other, detection of the redox current was poor in the recordings with the microelectrodes. Thus, only the data from three of the six guinea pigs were analyzed in this study.

Limit of detection (LOD) for *in vivo* measurements of the methylcobalamin concentration

An '*in vivo*' LOD value for each BDD microelectrode was obtained for every series of animal experiments as follows. In the cochlear perilymph and leg muscle of an individual guinea pig, a ten-minute recording of the microelectrode background current measured before methylcobalamin injection was extracted. Subsequently, the standard deviation (SD) of this current and the slope of the *in vitro* calibration curve for methylcobalamin were used to calculate the LOD value from the relationship [51]:

$$LOD = 3SD/slope \qquad \text{equation (1).}$$

Individual LOD values are plotted in Figure 4d and Figure S9(c)(f).

References

(45) Gonon, P.; Gheeraert, E.; Deneuville, A.; Fontaine, F. Characterization of heavily B-doped polycrystalline Raman spectroscopy and electron spin resonance. *J. Appl. Phys.* **1995**, *78*, 7059–7062.

(46) Asai, K.; Ivandini, T. A.; Einaga, Y. Continuous and selective measurement of oxytocin and vasopressin using boron-doped diamond electrodes. *Sci. Rep.* **2016**, *6*, 32429.

(47) Kilkenny, C.; Browne, W. J.; Cuthill, I. C.; Emerson, M.; Altman, D. G. Improving Bioscience Research Reporting: The ARRIVE Guidelines for Reporting Animal Research. *PLoS Biol.* **2010**, *8*, e1000412.

(48) Andrade, L. S.; Rocha-Filho, R. C.; Cass, Q. B.; Fatibello-Filho, O. Simultaneous Differential Pulse Voltammetric Determination of Sulfamethoxazole and Trimethoprim on a Boron-Doped Diamond Electrode. *Electroanalysis* **2009**, *21*, 1475–1480.

(49) Asai, K.; Ivandini, T. A.; Falah, M. M.; Einaga, Y. Surface Termination Effect of Boron-Doped Diamond on the Electrochemical Oxidation of Adenosine Phosphate. *Electroanalysis* **2016**, *28*, 177–182.

(50) Nin, F.; Hibino, H.; Doi, K.; Suzuki, T.; Hisa, Y.; Kurachi, Y. The endocochlear potential depends on two K+ diffusion potentials and an electrical barrier in the stria vascularis of the inner ear. *Proc. Natl. Acad. Sci. USA*. **2008**, *105*, 1751–1756.

(51) Shrivastava, A.; Gupta, V. B. Methods for the determination of limit of detection and limit of quantitation of the analytical methods. *Chronicles Young Sci.* **2011**, *2*, 21–25.

2. Supporting Figures (Figure S1-S12)

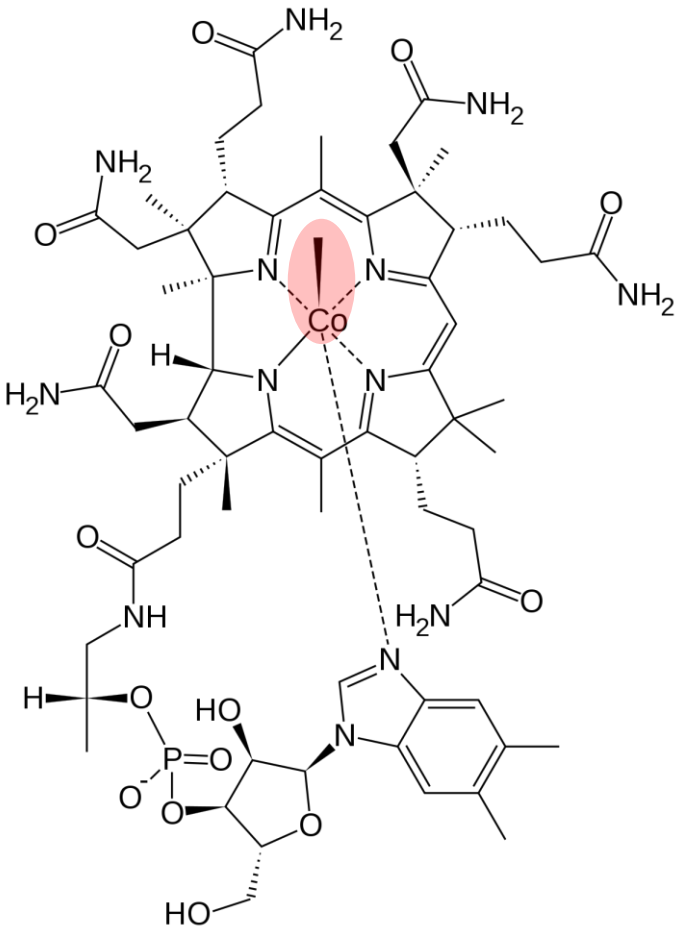

Figure S1 Chemical structure of methylcobalamin.

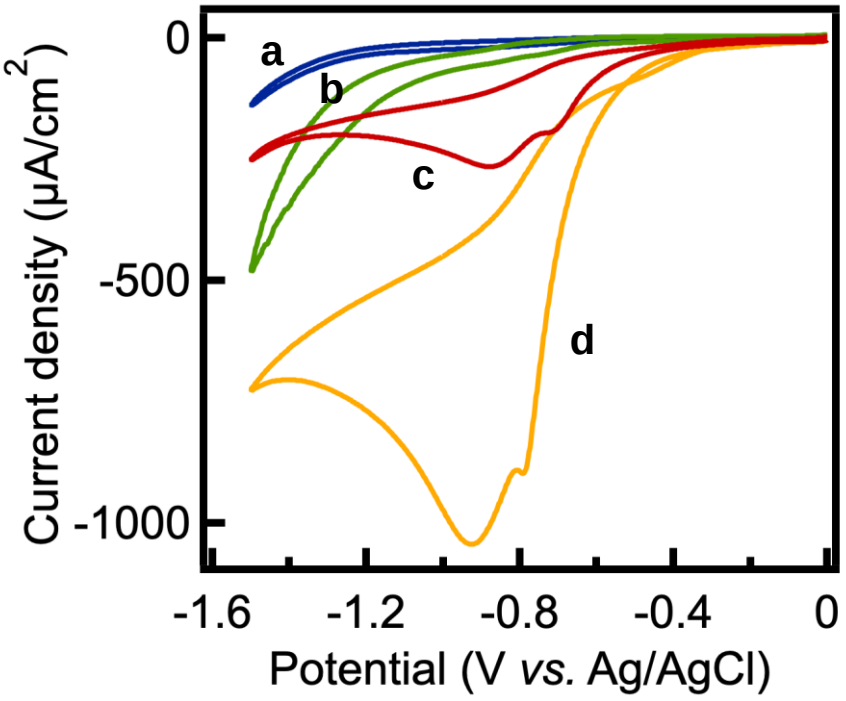

Figure S2. Cyclic voltammograms (CVs) of 0.1 M phosphate buffer (PB) solution in the absence and in the presence of 100 μM methylcobalamin at a scan rate of 0.1 V/s using a BDD plate electrode. (a) Absence of methylcobalamin (background) (degassed with nitrogen). (b) Presence of 100 μM methylcobalamin degassed with nitrogen. (c) Presence of 100 μM methylcobalamin in normal situation with dissolved oxygen. (d) Presence of 100 μM methylcobalamin with saturated oxygen.

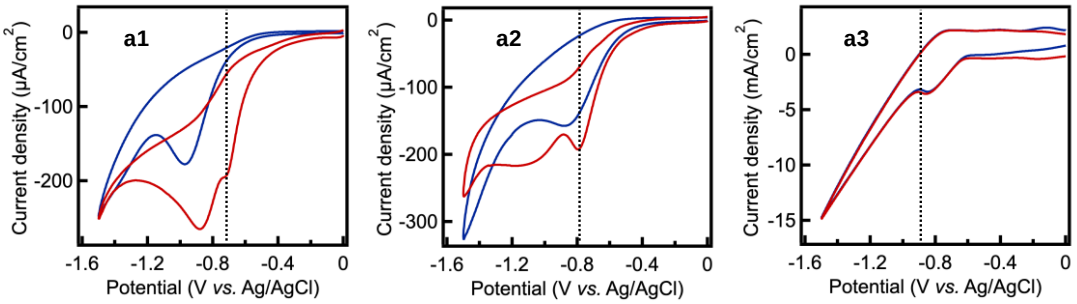

b

	Electrode		
	BDD	GC	Pt
S/B	4.7	1.4	1.1

Figure S3. Comparison between BDD, glassy carbon and Pt electrodes for detecting methylcobalamin. CVs obtained with a (a1) BDD plate electrode, (a2) glassy carbon (GC) plate electrode, and (a3) Pt plate electrode. Cyclic voltammograms (CVs) of 0.1 M phosphate buffer (PB) solution in the absence (blue) and in the presence (red) of 100 μM methylcobalamin were obtained. Scan rates were 0.1 V/s. The signal-to-background (S/B) ratios of the data obtained with the three electrodes are shown in (b). The ratios were calculated at the cathodic peak potential for methylcobalamin indicated by the dashed lines in (a1), (a2) and (a3).

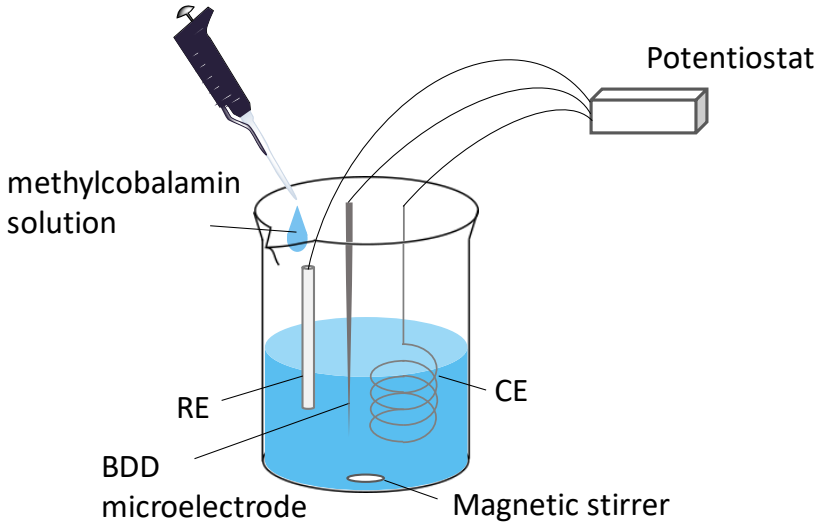

Figure S4. Continuous measurement setup for the calibration of BDD microelectrodes for the measurement of methylcobalamin. The BDD working electrode (WE), a Ag/AgCl reference electrode (RE) and a Pt wire counter electrode (CE) were placed in 5 ml of PB solution in a beaker. The current was recorded using a potentiostat (ALS 852 cs, BAS Inc., Japan). The methylcobalamin concentration in the beaker was increased in stages (1, 3, 10, 30, 100 nM) by sequentially adding drops of methylcobalamin stock solutions (1, 10, 100 μM methylcobalamin in PB) into it. The solution was stirred by a magnetic stirrer for 3 seconds just after each addition.

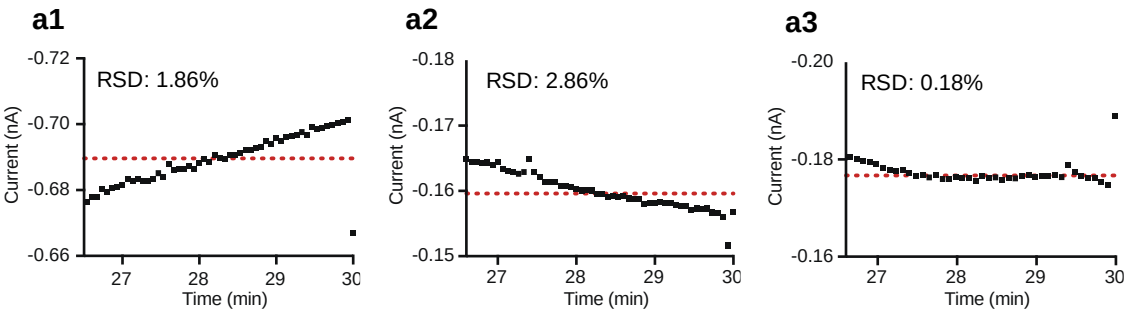

Figure S5. Stabilization of the background current for 200 s before adding the methylcobalamin. (a1) Protocol A, (a2) Protocol B, and (a3) Protocol C. The data were extracted from Fig. 2(a2), 2(b2), and 2(c2). The relative standard deviations (RSDs) of the background current are shown.

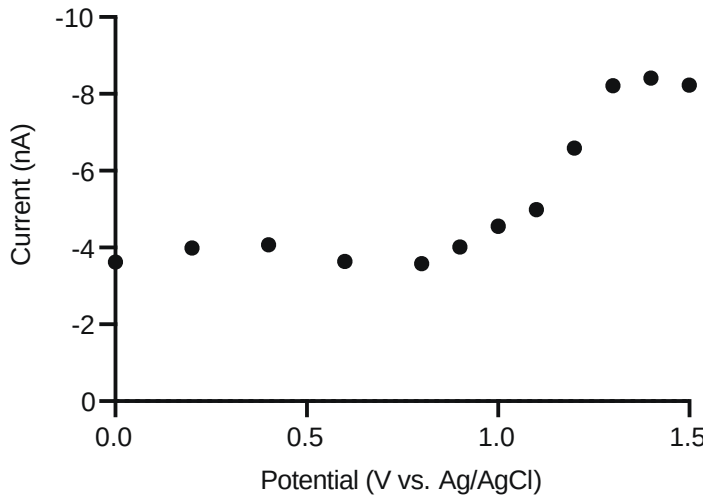

Figure S6. Optimization of the applied positive potential for Protocol C. CVs in the positive direction of a phosphate buffer (PB) solution in the presence of 100 μM methylcobalamin were performed using a plate BDD electrode. The scan rate was 0.1 V/s. The potential was scanned as follows: (Initial) 0.0 V (vs.Ag/AgCl) → (Applied positive potential) → −0.7 V (vs. Ag/AgCl). The horizontal axis shows the applied potential, and the vertical axis shows the methylcobalamin reduction current at −0.7 V (vs.Ag/AgCl) obtained from each CV.

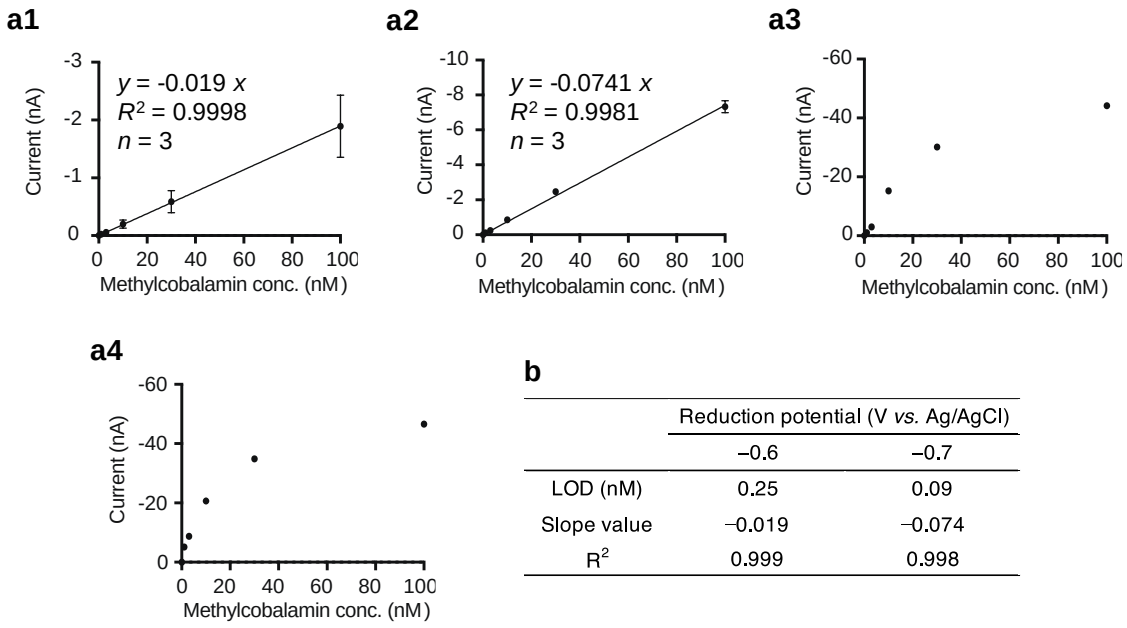

b

	Reduction potential (V *vs.* Ag/AgCl)	
	−0.6	−0.7
LOD (nM)	0.25	0.09
Slope value	−0.019	−0.074
R^2	0.999	0.998

c

Methylcobalamin conc.(nM)	Reduction potential (V *vs.* Ag/AgCl)			
	−0.6		−0.7	
	Current ± SD (nA)	RSD (%)	Current ± SD (nA)	RSD (%)
1	−0.024 ± 0.006	−24.4	−0.100 ± 0.007	−7.0
3	−0.056 ± 0.020	−35.0	−0.241 ± 0.014	−6.2
10	−0.199 ± 0.066	−33.4	−0.850 ± 0.014	−1.6
30	−0.586 ± 0.188	−32.1	−2.464 ± 0.102	−4.1
100	−1.891 ± 0.535	−28.3	−7.327 ± 0.332	−4.5

Figure S7. Optimization of the potential for methylcobalamin detection for Protocol C. The methylcobalamin detection potential was set to −0.6 V, −0.7 V, −0.8 V, and −1.0 V (vs.Ag/AgCl), and the calibration curves are shown in (a1), (a2), (a3), and (a4), respectively. (a1) and (a2) have linear calibration curves. The limit of detection (LOD), the slope and R^2 of the regression lines for (a1) and (a2) are shown in (b) and (c).

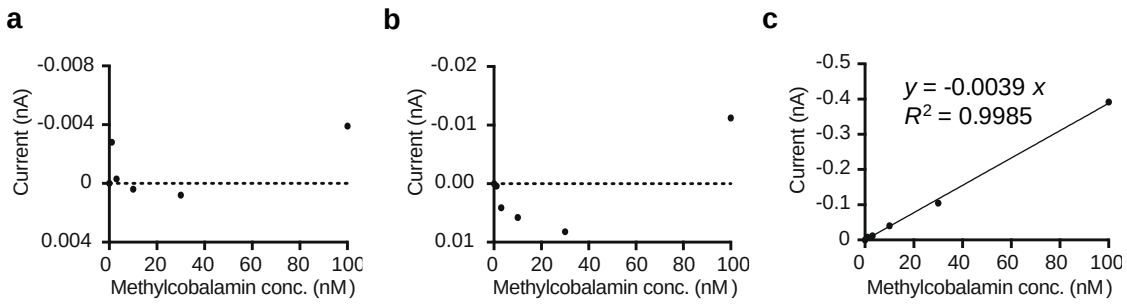

Figure S8. Optimization of the applied negative potential for Protocol C. The negative potential was set to −1.0 V, −1.5 V, and −2.0 V (vs. Ag/AgCl), and the calibration curves are shown in (a), (b), and (c), respectively. Only (c) has a linear calibration curve. The slope and R^2 of the regression line is also shown in (c).

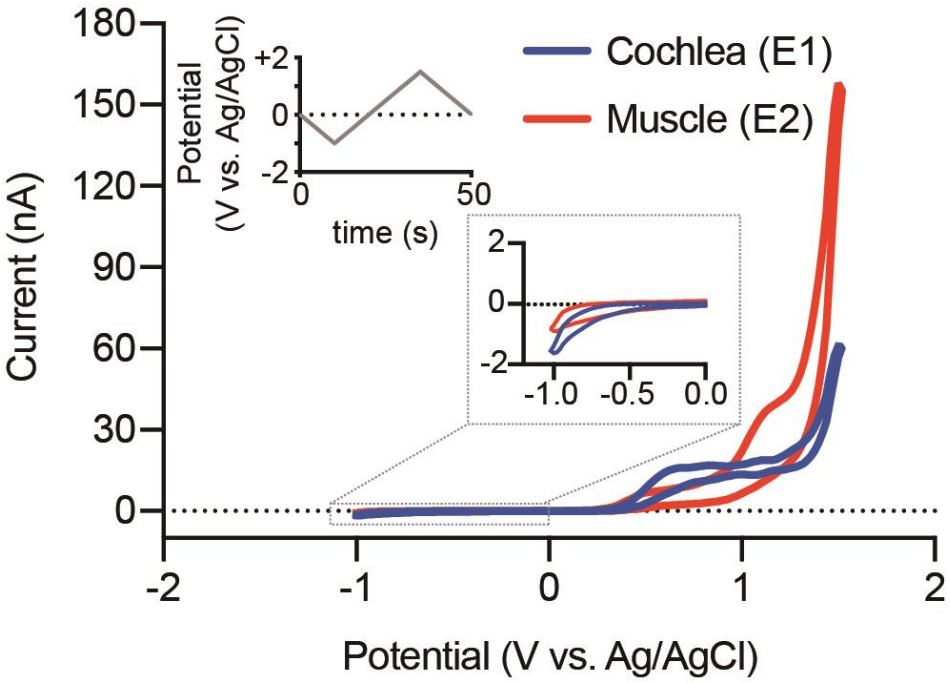

Figure S9. Electrochemical properties of the cochlea and leg muscle in a live guinea pig. The two BDD microelectrodes with the calibration curves shown in Figure 4b were inserted into the cochlear perilymph in the scala tympani (microelectrode E1) and the extracellular space in the gracilis muscle of the right hind leg (microelectrode E2) under controlled conditions. Then, cyclic voltammograms were measured with the voltage potential protocol shown in the inset (scan rate: 100 mV s^{-1}). The response in the cochlea and that in the leg are indicated by blue and red lines, respectively. Enlargement of the responses detected from 0 V to -1.0 V is shown in the *inset*.

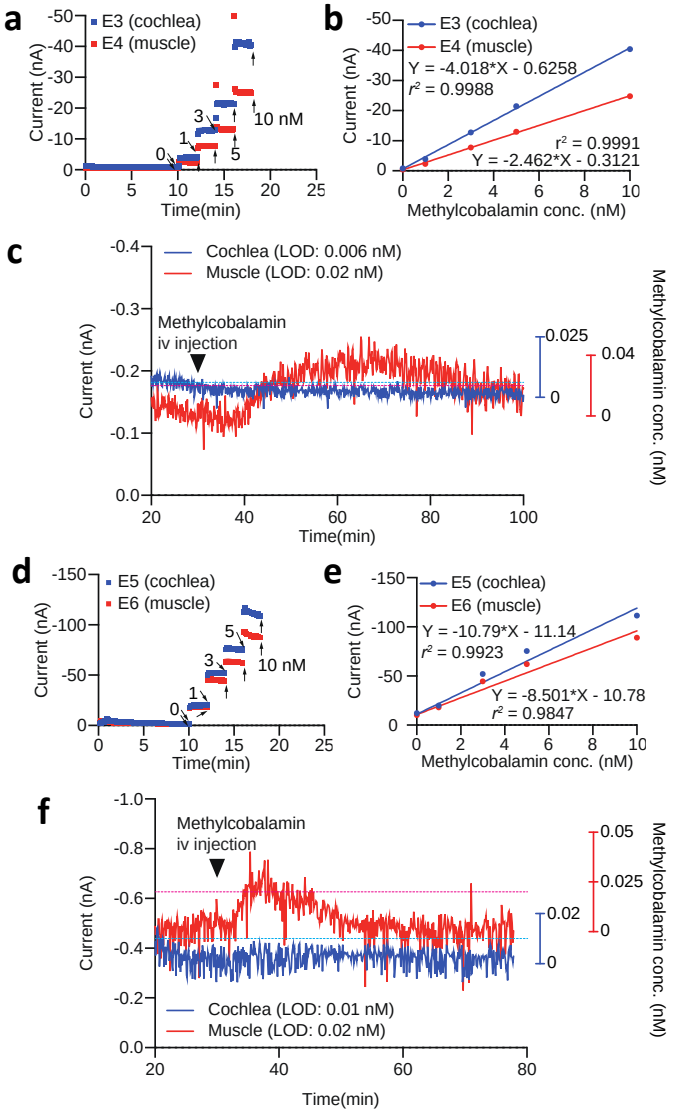

Figure S10. *In vivo* electrochemical detection of methylcobalamin in different guinea pigs. Two further anesthetized guinea pigs, not the one used for analysis shown in Figure 4, were examined with the *in vivo* microsensing system and the results are displayed in (a, b, c) and (d, e, f), respectively. In these two series of assays, four BDD microelectrodes in total were used (sensors E3 and E4 for the guinea pig in (a-c); microelectrodes E5 and E6 for the guinea pig in (d-f)). For the *in vitro* calibration (shown in (a, b) and (d, e)), each microelectrode was subjected to the same chronoamperometry protocol (Protocol C) shown in Figure 2(c1). In the recordings in (a, b) and (d, e), methylcobalamin (1−10 nM dissolved in phosphate buffer solution) was added incrementally to the electrolyte; the cathodic current at −0.7 V (vs. Ag/AgCl) for each methylcobalamin concentration was recorded. The steady-state current (shown by the arrows in (a) and (d)) is plotted against the drug concentration in (b) and (e), respectively. Values for the slope and r^2 of the regression line for each sensor are shown. Note that the slopes of the microelectrodes used in the cochlea (E3 and E5: blue) exceeded those used

for the leg (E4 and E6: red). In (c) and (f), each pair of calibrated microelectrodes was inserted into the cochlear perilymph (blue) and into the leg muscle (red); the cathodic current at −0.7 V (vs. Ag/AgCl) using Protocol C was monitored every 5 seconds. Methylcobalamin (MeCbl) at 10 mg kg^{-1} was intravenously injected into the guinea pigs 30 min (filled arrowhead) after starting recording. The methylcobalamin concentrations in the cochlea and muscle (blue and red axes on the right hand side, respectively) were obtained using the calibration curves in (b) and (e). The blue and red dotted lines indicate the '*in vivo*' limits of the detection values for each microelectrode (see 'Methods'); these values are displayed in (c) and (f).

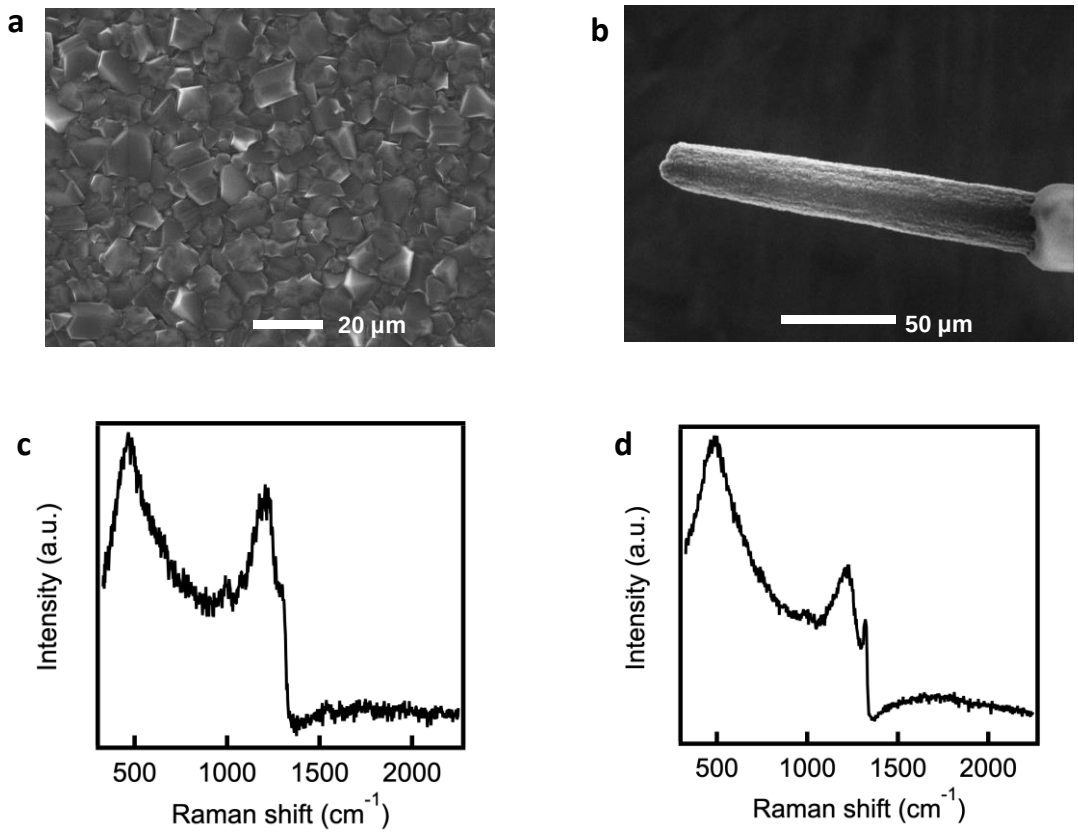

Figure S11. SEM images of (a) plate electrode and (b) microelectrode and Raman spectra of (c) plate electrode and (d) microelectrode.

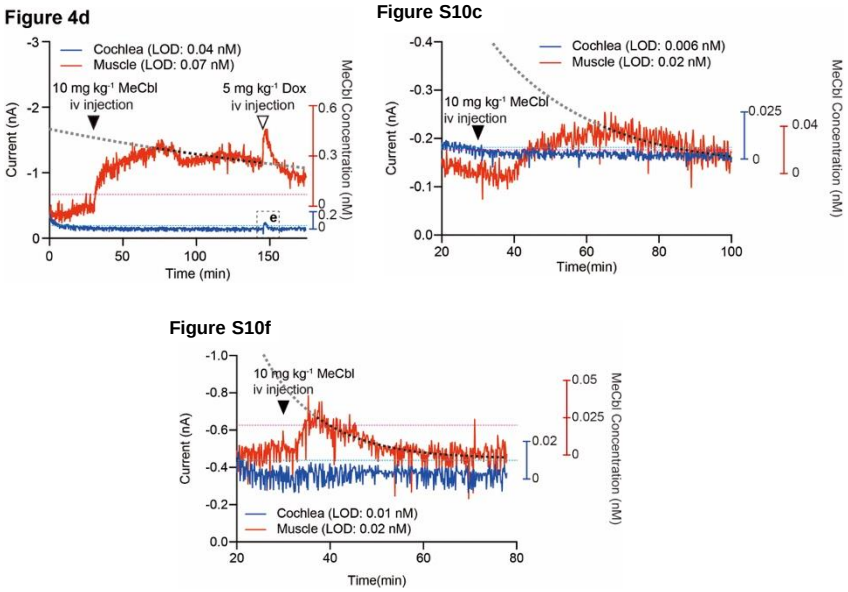

Figure S12. The broken lines in the three figures show the exponential fitting curves to obtain the half-life time for methylcobalamin concentrations in the leg muscles (for the values, see Table S1 in Supporting Information).

3. Supporting Scheme (Scheme S1)

Scheme S1. Possible mechanisms for reduction of methylcobalamin.

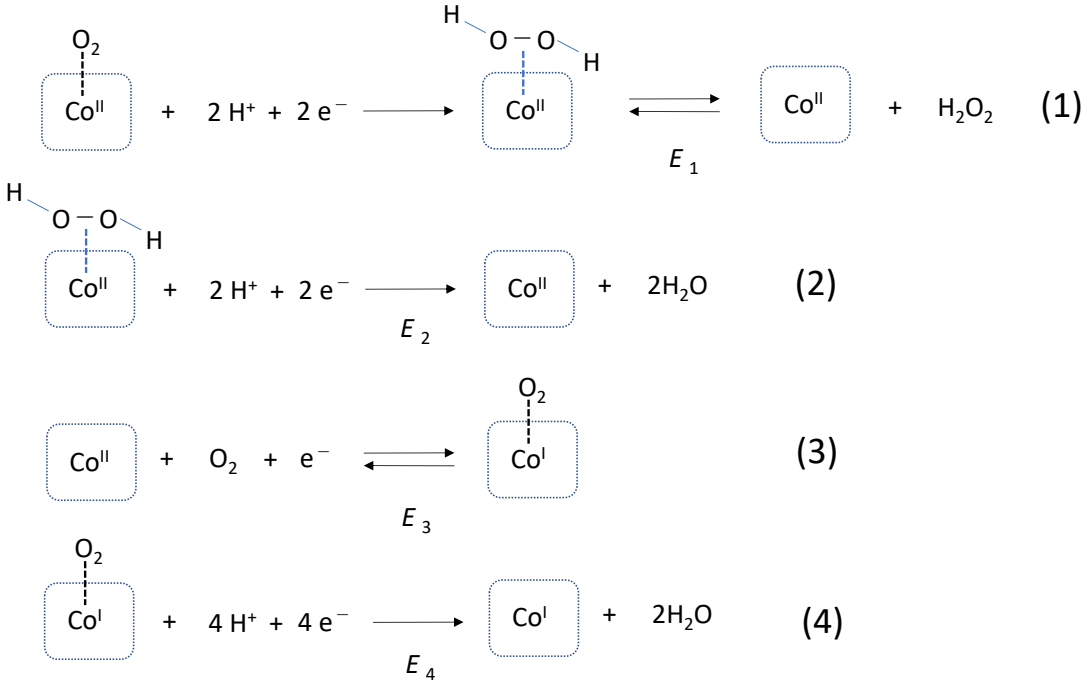

4. Discussion on pharmacokinetics

The declining kinetics of methylcobalamin in the leg muscle in Figure 4d is likely to be slower than the predicted kinetics in the plasma. We believe that this characteristic depends upon the property of the drug, due to the following reasoning. In Figure 4d, after examination of methylcobalamin, we subsequently administrated doxorubicin via a blood vessel to the same guinea pig and measured the responses with the same pair of the BDD microelectrodes. We detected a rapid decrease of the drug concentration with a half-life time ($t_{1/2}$) of 6.1 min in the muscle and with that of 2.4 min in the cochlea. Furthermore, in our earlier work, the BDD microelectrode succeeded in monitoring the behavior of bumetanide (30 mg kg^{-1} administration) with a $t_{1/2}$ of ~3.5 min in guinea-pig cochlea and that of ~8.65 min in rat brain.[24] These two lines of observations indicate that our method can very sensitively detect the declining phase with high time resolution. In addition, we previously found with the BDD microelectrode system that the response of antiepileptic agent, lamotrigine, showed slow kinetics (see Figure 6c in ref. 24), as observed in the results for methylcobalamin. Altogether, the pharmacokinetics measured in Figure 4d in the present study was likely to represent the native and real response of the drug.

We fitted the decline phase of the methylcobalamin concentrations measured in leg muscle of the three guinea pigs to a monophasic exponential decay model (Figures 4d, S10c, and S10f; see the Figure S12). Other pharmacokinetics parameters were also obtained and shown in Table S1 beneath the three panels. It is noteworthy that, the kinetics in the experiment of Figure S10f was characterized by relatively rapid time course (for instance, $t_{1/2}$ = ~7 min), as compared to the kinetics in other two experiments. Inconsistency of the pharmacokinetics amongst the animals may be due to variations in anatomical or morphological profiles such as a difference in distribution pattern of blood vessels. In this context, detectability for such a difference in the local responses is an advantage of our system, which has not yet been addressed by any existing conventional approaches.

It is true that comparison between the local kinetics and the plasma kinetics is informative. Nevertheless, it is technically impossible to indwell the BDD microelectrode in blood vessel for the reason that the electrode is not flexible enough. In addition, conventional methods such as LC-MS/MS have low sampling rates and thereby the data would not be comparable to the measurement with the BDD microelectrode. We will address this issue in the future work.

5. Supporting Table (Table S1)

Table S1. Pharmacokinetics of methylcobalamin in leg muscle

	Figure 4d	Figure S10c	Figure S10f
Peak concentration (C_{max}; nM)	0.407	0.047	0.032
Time to reach the maximum concentration (t_{max}; min)	46.3	35.1	8.54
Half-life time ($t_{1/2}$; min)	213	20.4	7.07